Cascade-free Doppler-tuned precision measurement of the lifetime of the $2\,^3S_1$ state in He-like niobium ($^{93}Nb^{39+}$)

A. Simionovici
Laboratoire Grenoblois de Recherches sur les Ions, les Plasmas et la Physique Atomique (LAGRIPPA), CENG, Boîte Postale 85X, Grenoble, France

B. B. Birkett and R. Marrus
Department of Physics, University of California, Berkeley, California 94720

P. Charles and P. Indelicato
Laboratoire de Physique Atomique et Nucléaire (LPAN), Institut de Radium, Université Pierre et Marie Curie, T12, Boîte 93, 75252 Paris, CEDEX 05, France

D. D. Dietrich
Lawrence Livermore National Laboratory, L-296, P. O. Box 808, Livermore, California 94550

K. Finlayson
Gesellschaft für Schwerionenforschung m.b.H., 6100 Darmstadt, Germany
(Received 19 October 1992; revised manuscript received 14 September 1993)

The lifetime of the $2\,^3S_1$ state in He-like niobium (Nb^{39+}) has been precisely determined with a beam-foil time-of-flight technique. The isotope ^{93}Nb ($I = \frac{9}{2}$) was chosen in order to minimize cascade effects through hyperfine quenching of the primary feeding state. Further precision was obtained by removing blends with a Doppler-tuned transmission filter. Other cascade contributions were analyzed and found to be negligible. The result is $45.45(16)\times10^{-12}$ sec and represents increased sensitivity to corrections of $O(Z\alpha)^2$ in the $Z\alpha$-series expansion for the lifetime by a factor of 5.

PACS number(s): 32.70.Fw, 32.30.Rj, 12.20.Fv, 31.30.Jv

The relativistic $M1$ decay of the $(1s)(2s)$ $(J = 1)$ $2\,^3S_1$ state to the $(1s^2)$ $1\,^1S_0$ ground state in heliumlike atoms is a relatively rare electromagnetic transition which has been studied quite extensively in low-Z atoms by a number of authors, both experimentally and theoretically. The relativistic transition is named as such because the nonrelativistic theoretical transition rate is zero, and so a relativistic formulation of the calculation must be used from the outset. Recent measurements [1,2] in high-Z ions have had sufficient precision to be sensitive to corrections of order $(Z\alpha)^2$ to the leading term in the series expansion for this lifetime. The uncertainties of these measurements have still been, however, larger than the 1–2 % precisions of the various theoretical calculations. For reviews see Refs. [3,4].

Measurements of this lifetime have thus far been limited to precisions of about 2–3 %. These precisions have been limited mainly by the presence of cascades of electrons from high Rydberg levels. These cascades may either repopulate the $2\,^3S_1$ state of interest from other n=2 states, as represented in Fig. 1 by thin solid lines, or they may give rise to transitions that are not completely resolved from the transition of interest. These possible blends from other $n = 2$ states are represented as dashed lines in Fig. 1. This experiment examined the $M1$ transition in He-like $^{93}Nb^{39+}$ where, by making use of previous experimental results, the undesired contributions due to cascades could be either eliminated or neglected. This has yielded a precise measurement of a lifetime of whose transition energy lies in the x-ray region. This measurement of the $2\,^3S_1$ lifetime also has the precision necessary to be sensitive to higher-order corrections in the predicted lifetime.

The experiment was conducted at the GANIL accelerator complex (Caen, France) on He-like Nb^{39+} ions

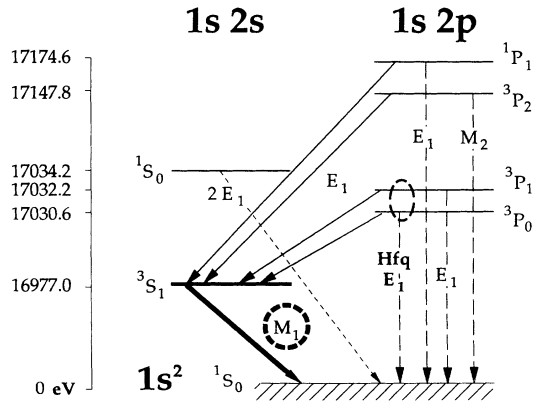

FIG. 1. Energy level diagram for He-like Nb^{39+}. Cascade transitions that repopulate the $2\,^3S_1$ level are represented by thin solid lines. Transitions that may cause blends with the transition of interest are shown as dashed lines.

with a beam energy of roughly 30 MeV/A, which corresponds to a decay length for the transition of interest of about 3.4 mm. The experimental apparatus, shown in Fig. 2 and previously described [1,5,6], consists of a time-of-flight spectrometer with two solid-state [Si(Li)] x-ray detectors. These detectors observe the radiation emitted from the excited ions downstream of the capture foil through collimating slit assemblies. These collimating slit assemblies have been designed so as to define spatial detection efficiencies which are insensitive to slightly varying detector-beamline distances. The first detector is positioned behind a slit assembly that is fixed in position with respect to the capture foil, and counts from this detector are used for normalization purposes. The second slit assembly is mounted to a precision translation stage (precision ≤ 1 μm), and the second detector is positioned behind this assembly. The detector is mounted to a separate translation stage, and is moved in parallel with the slit assembly such that the same portion of the detection crystal is used at each position. Data are obtained by measuring the ratio of counts in the movable detector to counts in the fixed detector as a function of position of the movable detector. Because of the relatively long decay length, small movements in the foil have little effect on the data and hence possible systematic effects are minimized. Precise measurement of the beam energy, as described elsewhere [1], yields a precision in the determination of the beam velocity and consequently of the lifetime of better than 5×10^{-4}. The final beam velocity was determined to be $\beta = v/c = 0.2474(1)$.

The flight path of the beam is controlled through the use of a beam tuning system which is achromatic in both angle and position. The actual position of the beam is monitored during the run through the use of highly precise diagnostics. These include several beam profilers which determine the position of the beam within the time-of-flight apparatus to within better than 0.5 mm and/or 0.25 mrad (1 mm at a distance 4 m away). The beam was seen to wander randomly between these limits during the run, and the effect of these small movements is reflected in the statistical uncertainty determined from the fit to the final decay curve.

Effects due to electron cascades from high Rydberg levels were eliminated or minimized by several means. Normally the greatest repopulation of the $2\,^3S_1$ state from within the $n = 2$ manifold is due to cascades through the $2\,^3P_0$ state (see Fig. 1), for the $2\,^3P_0$ state is metastable

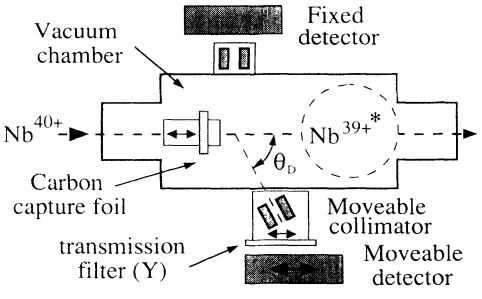

FIG. 2. Schematic design of experimental apparatus, including a Doppler-tuned transmission filter.

($\tau = 1.2\times10^{-9}$ sec) and the only allowed decay from this state is to the $2\,^3S_1$ state. Through the use of hyperfine quenching, however, the natural lifetime of the $2\,^3P_0$ state may be greatly reduced and another decay channel allowed [7]. The chosen isotope of Nb ($A = 93$) has a nonzero nuclear spin ($I = \frac{9}{2}$), which gives rise to hyperfine quenching of the $2\,^3P_0$ state by mixing it with the $2\,^3P_1$ state. The $2\,^3P_1$ state decays directly to the ground state with a lifetime of 4.1×10^{-16} sec, and hence through hyperfine mixing the $2\,^3P_0$ state may decay directly to the ground state as well. Strong quenching of the lifetime of the $2\,^3P_0$ state is made possible because the $2\,^3P_0$ and $2\,^3P_1$ states are relatively close ($\Delta E = 1.7$ eV), and the nuclear moment and spin combine to produce a strong coupling. Accurate calculations of hyperfine quenching have been done [7] and used for previous measurements in He-like Ag [5] and Gd [6]. In this case, with hyperfine quenching present the $2\,^3P_0$ state has a branching ratio of about 2×10^4 to the ground state compared to the $2\,^3P_0 \rightarrow 2\,^3S_1$ transition. The initial population of the $2\,^3P_0$ state thus decays directly to the ground state immediately after the foil, and any electrons that later cascade into this state from higher n levels are immediately channeled to the ground state as well.

Transitions from the $2\,^3P_2$ state may also repopulate the $2\,^3S_1$ state. The rate for this transition is 3.3×10^{10} sec^{-1}, which is roughly ten times smaller than the rate for the $2\,^3P_2 \rightarrow 1\,^1S_0$ transition to the ground state. Hence again the initial population of this state has largely decayed to the ground state within a short distance of the foil.

In order to estimate the repopulation of the $2\,^3S_1$ state due to cascades through the $2\,^3P_2$ state far from the foil, we have determined the number of counts in the semiresolved peak arising from the $2\,^1P_1 \rightarrow 1\,^1S_0$ and $2\,^3P_2 \rightarrow 1\,^1S_0$ transitions (see Fig. 3). To set an upper bound on the $2\,^3P_2 \rightarrow 2\,^3S_1$ repopulation rate, all of the counts in this semiresolved peak were assumed to come from the $2\,^3P_2 \rightarrow 1\,^1S_0$ transition, and were then multiplied by the known branching ratio of 0.121 for the transition $2\,^3P_2 \rightarrow 2\,^3S_1$ compared to $2\,^3P_2 \rightarrow 1\,^1S_0$. This number was then subtracted from the counts under the $2\,^3S_1 \rightarrow 1\,^1S_0$ peak

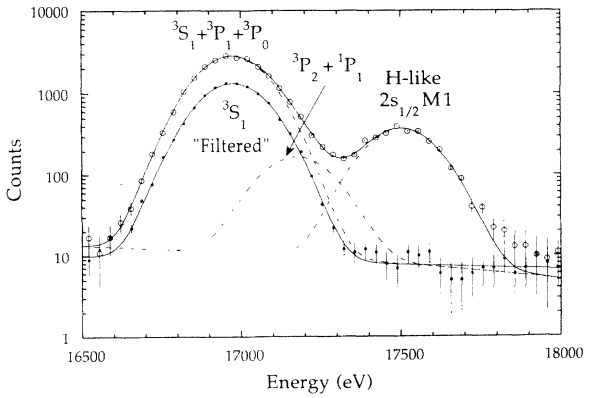

FIG. 3. Sample spectrum sensed by the movable detector 500 μm from the foil, taken with and without the yttrium Doppler-tuned transmission filter in place.

of interest. These subtracted counts were found to be approximately one-half of the standard deviation of the number of counts in the peak of interest, and as such are largely negligible.

The $2\,^3P_1$ and the $2\,^1P_1$ states, with lifetimes $\tau(2\,^3P_1)=1.2\times10^{-15}$ sec and $\tau(2\,^1P_1)=4.1\times10^{-16}$ sec, decay to the ground state immediately after the foil or, again, if repopulated downstream of the foil, give negligible contributions to the population of the $2\,^3S_1$ state due to branching ratios of 10^4–10^5 to the ground state.

Blends due to transitions from cascades passing through the $2\,^1P_1$, $2\,^3P_0$, $2\,^3P_1$, and $2\,^3P_2$ states to the $1\,^1S_0$ ground state present other possible systematic errors. While the $2\,^1P_1$ and $2\,^3P_2$ lines can be partially resolved from the $M1$ line of interest ($\Delta E \approx 200$ eV), the $2\,^3P_0 \rightarrow 1\,^1S_0$ and $2\,^3P_1 \rightarrow 1\,^1S_0$ transitions are unresolved by the detector ($\Delta E \approx 54$ eV), thus possibly contributing significantly to the measured $2\,^3S_1$ rate. In order to simply eliminate these four possible blends, we have used a technique developed by Schmieder and Marrus [8] known as "Doppler-tuned filtering." A thin yttrium foil, with known K-shell absorption edge $B_K = 17038$ eV, was placed in front of the movable detector in order to filter out the high energy side of the spectrum, namely, the $2\,^1P_1$, $2\,^3P_2$, $2\,^3P_1$, and $2\,^3P_0$ lines discussed above. The energy matching of this filter was critical, for the $2\,^3P_0$ and the $2\,^3S_1$ lines are only separated by about 54 eV, while the Doppler width due to the angular acceptance of the collimating slits was approximately 12 eV. A linear Doppler shift associated with a vision angle of 82.2° with respect to the beam (see Fig. 2) was used in order to appropriately shift the energies of these transitions above the K edge, so that with a 100-μm yttrium foil the transmission coefficient for the $2\,^3P_0 \rightarrow 1\,^1S_0$ decay was roughly 60 times smaller than that for the $2\,^3S_1 \rightarrow 1\,^1S_0$ decay. The result of this filtering is shown in Fig. 3 for a sample spectrum taken at a distance of 500 μm from the foil. The high energy side of the spectrum is clearly greatly reduced, demonstrating the elimination of the blends from the $2\,^1P_1$, $2\,^3P_1$, $2\,^3P_0$, and $2\,^3P_2$ states. The H-like $M1$ $2s_{1/2}$-$1s_{1/2}$ line, produced by excitation in the foil of the H-like beam, is also clearly reduced in the spectrum.

Finally, direct repopulation of the $2\,^3S_1$ state from $n = 3$ or higher states does not seem to occur since neither the dominant $n = 3$ to $n = 1$ nor the $n = 3$ to $n = 2$ lines are observed in the experimental spectrum.

Each spectrum from both the movable and fixed detectors was fitted with a single Gaussian curve and a linear background. A first decay curve was formed from data taken without the yttrium filter in place in order to estimate the contributions due to blends. A single exponential fit yielded a lifetime $\tau(2\,^3S_1)=44.76(39)\times10^{-12}$ sec with a reduced χ^2 of 4.43. The uncertainty is statistical only and has been taken at the 1σ confidence limit.

A final decay curve was formed with data taken with the Y filter in place, which removed all blends from the higher $(1s)(2p)$ states as shown in Fig. 3. This filtering procedure produced remarkably pure $2\,^3S_1$ lines at each position of the movable detector, so that a single exponential without any background could be fit exceptionally well to the data. The data and fit obtained using this method are shown in Fig. 4, along with a plot of the fit residuals ($= y_{\rm data} - y_{\rm fit}$). This fit yielded the final result $\tau_{\rm exp}(2\,^3S_1) = 45.45(16) \times 10^{-12}$ sec, a precision of 0.35%, with an improved reduced χ^2 of 2.0. Again the uncertainty is statistical only and has been taken at the 1σ confidence limit. The final quoted uncertainty has been increased to correct for the reduced χ^2 being larger than one. An independent estimate of the uncertainty has been obtained through the use of the "bootstrap method" [9,10]. The value obtained using the bootstrap method on the residuals and the above quoted uncertainty generated from the corrected covariance estimates agree to within 5%, providing confidence in the statistical significance of the value.

In order to test for sensitivity to foil bowing during the run, several points were repeated and in general the curve was sampled in both increasing and decreasing distances from the foil. Also, we have attempted to account for possible cascades by fitting the data to an exponential plus a power law, or to the sum of two exponentials. Both of these have proven unfeasible, again providing confidence that the cascade contributions have been removed experimentally.

A possible apparent periodic oscillation of the data about the exponential decay curve may be identified in Fig. 4. The period of this oscillation would be approximately 2.8 mm. Attempts to equate this oscillation to effects due to a "zero field quantum beat" [11] have proven unsuccessful, as the hyperfine splitting of the $2\,^3S_1$ level gives rise to a beat frequency which is at least three orders of magnitude too small. We further believe that any stray electric or magnetic fields present in our experimental apparatus are of too small a magnitude to produce such an effect. Mechanical causes cannot be completely

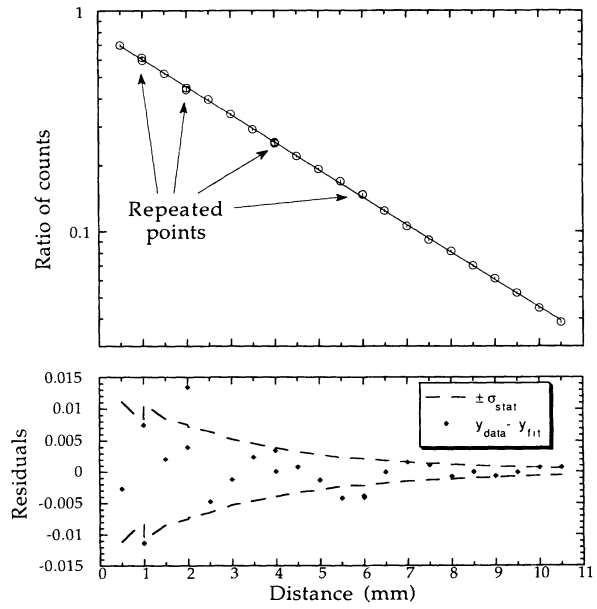

FIG. 4. Final data taken with yttrium filter in place, fitted to a single exponential, and fit residuals ($= y_{\rm data} - y_{\rm fit}$).

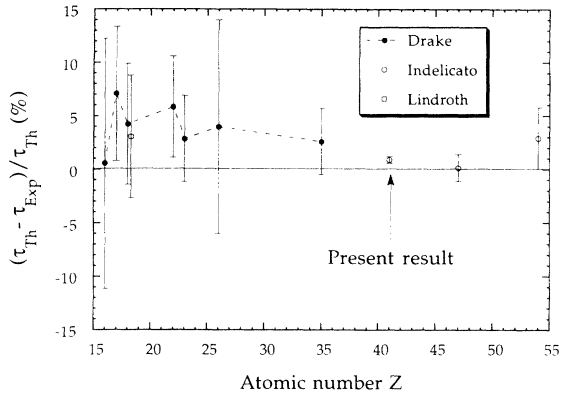

FIG. 5. Comparison of current body of experimental and theoretical results for the $2\,^3S_1$ lifetime. Experimental references: $Z = 16$, 17 [14]; $Z = 18$ [15]; $Z = 22$ [16]; $Z = 23$, 26 [17]; $Z = 35$ [2]; $Z = 47$ [18]; $Z = 54$ [1]. Theoretical references: $Z = 16$, 17, 22, 23, 26 [13]; $Z = 18$ [19]; $Z = 35$ [20]; $Z = 47$ [5]; $Z = 54$ [21].

ruled out. However, the influence of this possible oscillation is in the end negligible: when the data is fit to the convolution of an exponential and a cosine function, the resulting decay constant is found to change by less than one-tenth of our quoted uncertainty.

The body of existing experimental results as compared to theory is shown in Fig. 5. The current experimental value, at $Z = 41$, has the highest precision thus far obtained in the x-ray region. In Table I, a comparison is made between the experimental value and a theoretical value obtained from the multiconfiguration Dirac-Fock (MCDF) method by Indelicato. We note a 3σ or roughly 1% difference from the MCDF value, which has an estimated uncertainty of 1%. Sucher [4] has given an approximate series expansion including terms up to $(Z\alpha)^2$ for the $M1$ transition rate:

TABLE I. Experimental result and comparison with theory (values in psec).

	Experiment	MCDF method
$\tau(2\,^3S_1)$	45.45(16)	45.888

$$A(2\,^3S_1 \to 1\,^1S_0) \approx \tfrac{2}{3}\tfrac{\alpha(Z\alpha)^{10}m}{972}\{1 - \tfrac{4.1}{Z} + \tfrac{6.7}{Z^2} + c_2(Z\alpha)^2\}. \quad (1)$$

The coefficient for the $(Z\alpha)^2$ term, c_2, has been calculated by Lin [12] to be 1.07, and thus this term contributes 9.6% to the $M1$ rate at $Z = 41$. We note that the roughly 0.35% precision of this experimental result makes this the first measured lifetime with sensitivity to terms of order greater than $(Z\alpha)^2$.

This work was supported by NSF Grant No. PHY 9100505, by NATO Grant No. CRG 900630, and by the CNRS, France. This work was also performed under the auspices of the U.S. Department of Energy by LLNL under Contract No. W-7405-Eng-48. LAGRIPPA is Unité Mixte de Recherche du CNRS No. 038, and LPAN is Unité Associée au CNRS No. 771. The authors would like to thank the GANIL staff who provided excellent conditions for this experiment.

[1] R. Marrus, P. Charles, P. Indelicato, L. de Billy, C. Tazi, J. P. Briand, A. Simionovici, D. D. Dietrich, F. Bosch, and D. Liesen, Phys. Rev. A **39**, 3725 (1989).
[2] R. W. Dunford, D. A. Church, C. J. Liu, H. G. Berry, M. L. Raphaelian, M. Hass, and L. J. Curtis, Phys. Rev. A **41**, 4109 (1990).
[3] R. Marrus and P. J. Mohr, Adv. At. Mol. Phys. **41**, 181 (1978).
[4] J. Sucher, in *Proceedings of the Fifth International Conference on Atomic Physics, Berkeley, 1976,* edited by R. Marrus, M. Prior, and H. Shugart (Plenum, New York, 1977), p. 415.
[5] R. Marrus, A. Simionovici, P. Indelicato, D. D. Dietrich, P. Charles, J. P. Briand, K. Finlayson, F. Bosch, D. Liesen, and F. Parente, Phys. Rev. Lett. **63**, 502 (1989).
[6] P. Indelicato, B. B. Birkett, J. P. Briand, P. Charles, D. D. Dietrich, R. Marrus, and A. Simionovici, Phys. Rev. Lett. **68**, 1307 (1992).
[7] P. Indelicato, F. Parente, and R. Marrus, Phys. Rev. A **40**, 3505 (1989).
[8] R. W. Schmieder and R. Marrus, Nucl. Instrum. Methods **110**, 459 (1973); R. W. Schmieder, Rev. Sci. Instrum. **45**, 687 (1974).
[9] B. Efron, Stat. Sci. **1**, 54 (1986).
[10] G. Simpson, Astron. Astrophys. **162**, 340 (1986).
[11] H. J. Andrä, in *Progress in Atomic Spectroscopy,* edited by W. Hanle and H. Kleinpoppen (Plenum, New York, 1979), p. 829.
[12] D. L. Lin, Ph.D. dissertation, Columbia University, 1975.
[13] G. W. F. Drake, Phys. Rev. A **3**, 908 (1971).
[14] J. A. Bednar, C. L. Cocke, B. Curnutte, and R. Randall, Phys. Rev. A **11**, 460 (1975).
[15] G. Hübricht and E. Träbert, Z. Phys. D **7**, 243 (1987).
[16] H. Gould, R. Marrus, and R. W. Schmieder, Phys. Rev. Lett. **31**, 504 (1973).
[17] H. Gould, R. Marrus, and P. Mohr, Phys. Rev. A **33**, 676 (1974).
[18] B. B. Birkett, J. P. Briand, P. Charles, D. D. Dietrich, K. Finlayson, P. Indelicato, D. Liesen, R. Marrus, and A. Simionovici, Phys. Rev. A **47**, 2454 (1993).
[19] E. Lindroth and S. Salomonson, Phys. Rev. A **41**, 4659 (1990).
[20] The theoretical value for $Z = 35$, published in [2], is from a nonrelativistic calculation by Drake [13] which has been corrected for lowest-order relativistic effects by multiplying by the factor $[1 + 1.07(Z\alpha)^2]$.
[21] The theoretical value for $Z = 54$ is the MCDF Coulomb self-consistent value published in Ref. [1].

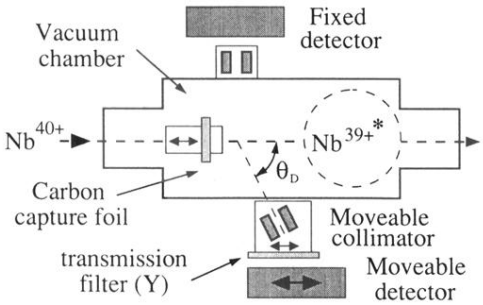

FIG. 2. Schematic design of experimental apparatus, including a Doppler-tuned transmission filter.